Review Article

Institution of MECHANICAL ENGINEERS
Journal of RAIL AND RAPID TRANSIT

Proc IMechE Part F:
J Rail and Rapid Transit
2023, Vol. 237(10) 1245–1259

DOI: 10.1177/09544097231156730
journals.sagepub.com/home/pif
Sage

Wheel-rail contact and friction models: A review of recent advances

Congcong Fang[1,2,3], Sulaiman A Jaafar[1,2,3], Wei Zhou[1,2,3], Hongkai Yan[1,2,3,4], Jun Chen[4] and Xianghui Meng[5]

Abstract

Rail transportation is regarded as a reliable, quick, and secure mode of transportation. The wheel-rail contact interaction is crucial to the railway operation since it is responsible for supporting, traction, braking, and steering of railway vehicles. Improper wheel-rail interactions may produce or exacerbate wheel-rail interface issues such as rolling contact fatigue (RCF) and wear, which can threaten the vehicle's running safety and stability. A review of the evolution and recent literature on wheel-rail contact mechanics and tribology is presented here. Topics covered include the basics of wheel-rail contact problem and methodologies for modeling both the normal contact (Hertzian and non-Hertzian) and tangential contact (Kalker's theories including CONTACT and FASTSIM algorithms, Polach's theory, USETAB program, etc.). The paper also reviewed various effects of contaminants and environmental conditions (water, leaves, sand, temperature, humidity, etc.) in wheel-rail contact. Various wheel-rail empirical adhesion models like the Water-induced low adhesion creep force model (WILAC) model and adhesion models based on elastohydrodynamic lubrication (EHL) theory (Greenwood-Tripp [GT] and Greenwood-Williamson [GW] models) are also reviewed. Lastly, the paper discusses the need and challenges for developing and integrating the wheel-rail non-Hertz contact model and adhesion model, as well as open areas for further research.

Keywords

Wheel-rail contact, creep force, adhesion model, contaminants, tribology

Date received: 22 July 2022; accepted: 24 January 2023

Introduction

Railways have been widely recognized as a fast, reliable, and secure form of transportation. Low energy consumption, environmental preservation, and higher security are among its most significant advantages. Railway vehicles are supported by high wheel-rail contact stresses within a coin-size area of the contact patch. The contact and resultant friction forces between the wheel and rail dominate the vehicles' steering, traction, and braking. The wheel-rail contact is also prone to various problems like wear, rolling contact fatigue (RCF), etc. Thus, accurate and efficient wheel-rail contact models are essential and hot topics in vehicle dynamic simulations and railway engineering science.

In general, wheel-rail contact problems can be divided into two categories; tangential and normal problems, which are solved sequentially.[1] For the normal contact problem, fast algorithms represented by Hertz-based analytical methods are commonly used in multibody dynamic code to evaluate wheel-rail contact force and contact patch. However, as a result of irregular and complicated contact geometries between wheel and rail, multi-point, conformal contact states are always involved, which are very difficult to be handled by the Hertzian analytical approach. In most models, creepage is important for determining creep forces in tangential contact problems. The evaluation of creep force and moments is complicated by longitudinal creepage, lateral creepage, spin creepage, and their cross-couplings.[2] In addition, the adhesion and slip areas of the contact patch must be determined to estimate the creep forces at the wheel-rail interface in various models. In recent decades, models addressing these problems have been developed. This article will focus on these models.

So far, most investigations on the wheel-rail creep force are formulated on dry contact and Coulomb's friction law assumptions. However, the wheel-rail contact pair is an

[1]Key Laboratory of Traffic Safety on Track, Ministry of Education, School of Traffic & Transportation Engineering, Central South University, Changsha, China
[2]Joint International Research Laboratory of Key Technology for Rail Traffic Safety, Changsha, China
[3]National & Local Joint Engineering Research Centre of Safety Technology for Rail Vehicle, School of Traffic & Transportation Engineering, Central South University, Changsha, China
[4]Institute of Science & Technology of the China Railway Urumqi Group Co., Ltd., Urumqi, China
[5]School of Mechanical Engineering, Shanghai Jiao Tong University, Shanghai, China

Corresponding author:
Wei Zhou, School of Traffic & Transportation Engineering, Central South University, 22 Shaoshan South Road, Tianxin District, Changsha 410075, Hunan, China.
Email: zhou_wei000@126.com

open tribological system that is subjected to contaminants such as sand particles, dirt, ice, rain, leaves, etc., or lubricants such as grease or oil added to the wheel-rail surface to reduce wear and friction between the wheel flange and the rail gauge face when a train negotiates a curved track.[3] Since all of these factors affect the tribological properties of the wheel-rail, therefore, adhesion models considering the third-body layers should also be a matter of concern.

Some earlier reviews have been done by Jacobson and Kalker,[4] focusing on the rolling contact theory. Knothe et al.[5] worked on these theories and integrated them into vehicle dynamics simulation. Piotrowski and Chollet[6] reviewed non-Hertzian wheel-rail contact models including multi-point contact models. In their review, Meymand et al.[7] compared the functionality of wheel-rail contact models by discussing the simplifying assumptions used in their development. Several reviews have been done on wheel-rail tribology. Olofsson and Yezhe[8] presented a literature review on experimental research on wheel-rail tribology under natural and artificial contaminants. Soleimani and Moavenian[9] also reviewed the same topic considering the effect of RCF. Foo et al.[10] reviewed wheel-rail interface friction management considering the effect of traction and braking. Recently, Vollebregt et al.[11] conducted a literature review on the understanding and modeling of wheel-rail creep forces, including the measurement method and modeling approach. The published review papers mostly focus on the wheel-rail problem from the single discipline of contact mechanics, tribology, or dynamics. The current work summarizes pioneering research and recent advances in wheel-rail contact analysis and friction models, focusing particularly on the integration of traditional dry wheel-rail contact models and adhesion contact models for the third-body layers.

The work begins by providing an overview of wheel-rail contact, then explores methods to analyze wheel-rail contact, including various contact models, creepage characteristics, detailed numerical analysis methods are described, effects of contaminants on the adhesion at the wheel-rail contact are explored, and various numerical models for adhesion are reviewed and, ultimately, a summary is provided, and limitations of the present studies and future research directions are analyzed.

Wheel-rail normal contact

Wheel-rail contact problem

Early contributions to wheel-rail contact theory include Carter's creep force law,[12] then Vermeulen and Johnson,[13] and then Kalker[14] who provided the framework for an accurate description. The wheel and rail have two main contact points:

a. The contact between the railhead and the wheel tread most often occurs on straight tracks due to little slip in straight lines and moderate arcs.
b. The contact between the wheel flange and the rail gauge most often occurs on sharp curves. This region is crucial in determining the wheel-rail life.[9,15] Here, two types of contact points exist, single-point and double-point contacts as shown in Figure 1(a) and (b).

The obvious way to solve a contact problem is to utilize numerical simulation like the Finite Element Method (FEM) and the Boundary Element Method (BEM) have been used to solve many rolling contact problems. They are addressed in Numerical simulation method of the paper.

The contact between wheel and rail is presumed to be quasi-identical and quasi-elastic where stress concentration occurs.[16] The stress problem involves both normal and tangential loads. Generally, the corresponding normal and shear stress distributions are not independent. However, due to the quasi-identical properties of the contact bodies, the normal contact can be decoupled from the tangential contact under a non-conformal contact condition which greatly simplifies the problem. Thus, the wheel-rail contact problem is normally treated separately in normal and tangential directions. The next section will deal with both Hertzian and non-Hertzian normal contact models in detail.

The Hertz contact theory

The normal contact problem is an overall term for the case of two elastic bodies pressed together under a normal force. The aim is to find the characteristic properties of the contact such as displacements, pressure distribution, penetration, and size and shape of the resulting contact patch.

According to Hertz,[17] when two bodies are pressed together based on the assumptions that; classical elasticity theory applies, constant curvatures inside the contact patch, the surface is infinitely large half-spaces, and there is a large radius of curvature in comparison to the contact size. Following that, the contact surface is assumed to be flat and elliptical with the pressure distribution semi-ellipsoid. Hertz's theory is extensively used to study wheel-rail contact mechanics and dynamics despite its limitation of only considering frictionless contact. Timoshenko and Goodier[18] and Hamilton[19] used this theory and improved it by incorporating the effects of traction and creepage. The major limitations of their theory are the assumptions of only one contact point with constant curvatures and the ellipse semi-axes being small in comparison to the radius of curvature at the contact point in wheel-rail contact. Hertzian contact patch dimensions are often inaccurate representations of actual contact shapes of the wheel-rail contact because the pressure distribution and elliptical contact patch obtained are not realistic. To better explain the wheel-rail normal contact, various non-Hertzian and semi-Hertzian contact theories are proposed.[6] They are discussed further in the following section.

The non-Hertz contact theory

The Kalker's non-Hertzian models. Kalker's exact (3D) rolling contact theory[20] is regarded as the most accurate wheel-rail contact theory. It is a BEM applied to problems involving non-Hertzian contact geometries, rolling contact problems in transient and steady-state, and linear elastic or viscoelastic bodies. The theory can also be used to solve

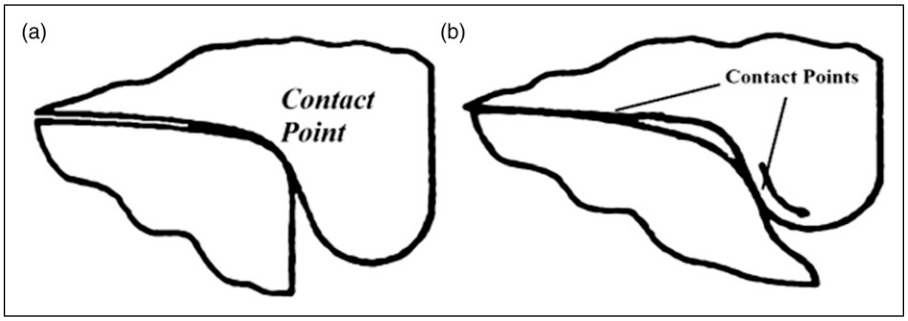

Figure 1. Contact status of the wheel-rail system[9]; (a) single-point contact; (b) two-point contact.

tangential contact problems and has been used in several studies involving wheel-rail contact mechanics.[21–23] Like Hertz's theory, Kalker's exact (3D) theory describes wheel and rail as infinitely large half-spaces with a large radius curvature relative to the contact area. The theory can handle non-elliptic and multi-contact patch cases. The theory has been elaborated in Tangential contact models of this paper.

Multi-Hertzian models. Multi-Hertzian methods are used in railway codes to calculate the elastic normal forces of wheel-rail contacts. These techniques can be effectively used to determine the forces of multiple elliptical simultaneous contacts. Additionally, they can be used to approximate the normal forces of non-elliptical patches as a sum of Hertzian contacts. In the multi-Hertzian model, Hertzian ellipses are used to represent interfaces between contacting bodies. The multi-Hertzian theory has been applied to several wheel-rail contact analyses. Pascal and Sauvage[24] realized the existence of secondary contact points from the sudden 'jump' of the wheelset during lateral displacement. The contact points represent a separate contact patch. The curvature value of each contact patch is used to calculate multiple contact ellipses for multi-Hertzian contact calculations. Ayasse et al.[25] proposed pre-calculated tables and an analytical formulation of the 'jump' for simplifying the multi-Hertzian contact calculations. Pascal and Soua[26] used multi-Hertzian techniques to solve normal contact problems in conformal contact situations. A multi-Hertzian model considering plasticity was developed by Sebès et al.[27] which shows contact stresses are consistent with perfect plasticity similar to the Semi-Hertzian model they developed in ref. 28.

Virtual penetration models. In these models, non-Hertzian normal contact problems are solved in a simplified, fast, and efficient manner by neglecting normal elastic deformations. The wheel and rail are regarded as bodies that revolve and rigidly penetrate each other. To solve the problems of low efficiency of CONTACT, researchers have presented different approximate virtual penetration models concerning wheel-rail contact including, the Kik–Piotrowski model,[6,29] the extended Kik–Piotrowski (EKP) model,[30] the modified Kik–Piotrowski (MKP) model,[31,32] the Ayasse-Chollet model (STRIPES),[33] the Linder model,[34] and the Shichani (ANALYN) model.[35] They can be used to solve both normal and tangential contact problems.

The Kik–Piotrowski model[29] is a non-iterative solution for the normal contact problem that involves estimating the contact patch analytically by ignoring surface deformation calculations. There have been several improvements to the KP model in terms of speed and robustness; Liu et al.[30] extended the KP model (called the extended Kik–Piotrowski (EKP) model) to include the effect of wheel-set yaw angle against the rail and variation in profile curvature across the contact patch. Sun et al.[31] presented a modified Kik-Piotrowski model (MKP) that accounts for the interaction between elastic deformation and normal pressure distribution.

The material surface deformation at the wheel-rail contact region was not considered in the virtual penetration method. As such, the virtual penetration method major-minor half-axis ratios of equivalent ellipses was found by Ayasse andChollet[33] to be different from the Hertzian contact theory. To solve the problem, they presented two methods for modifying longitudinal and lateral relative wheel-rail curvatures. The first method involves only modifying the longitudinal relative curvature and smoothing the lateral relative curvature, and the second method involves both longitudinal and lateral relative curvatures being modified.

The conversion ratio between the approach of wheel and rail contact bodies and virtual penetration is a constant value for the virtual penetration method. The value was set to 0.55 for the Kik-Piotrowski and Ayasse-Chollet approaches thus influencing the accuracy of the calculation. As a result, Sichani et al.[35] presented a novel approach taking into account surface material deformation of wheel-rail contact regions to accurately calculate wheel-rail permeability (Figure 2).

Table 1 summarizes some important papers on the wheel-rail Hertzian, non-Hertzian, multi-Hertzian, and virtual penetration contact models. It can be seen from the table that the contact models have roughly experienced Hertzian, Multi-Hertzian, and Non-Hertzian development stages. The Hertzian normal contact model is currently the most popular method because of its low computational cost and convenient implementation in multibody dynamic code. However, the Hertzian contact theory is not able to deal with the conformal and multi-point contact problems that frequently occur in the vicinity of the wheel flange regions. Exact non-Hertzian and numerical contact methods are computationally expensive when used in vehicle system dynamic analysis. Multi-Hertzian and virtual penetration models are the compromise between the Hertzian and exact non-Hertzian methods in terms of computational accuracy and efficiency.

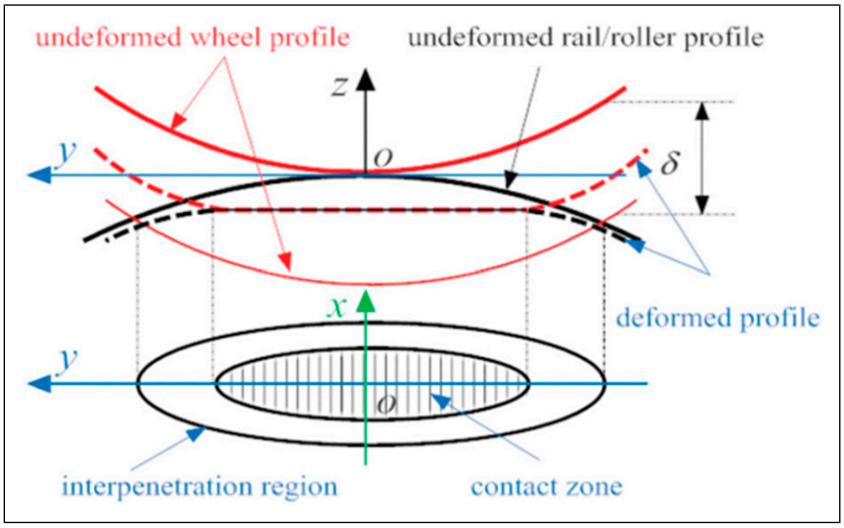

Figure 2. The interpenetration region and the contact zone.[36]

Table 1. Summary of published papers on wheel-rail contact.

Reference	Type of contact problem	Contact model
Carter's creep force law,[12] Vermeulen and Johnson,[13] and Kalker[14]	Theoretical contact	Early theoretical contact
Hertz[17]	Hertzian normal contact models	Model for calculating contact area and the normal pressure distribution
Timoshenko and Goodier[18] and Hamilton[19]	Hertzian normal contact models	Modify and improve the Hertz model by considering the effects of traction and creepage
Kalker's exact (3D) rolling contact theory[37]	Non-Hertzian normal contact models, tangential contact.	Implemented in software CONTACT
Li-Kalker theory,[38,39]	Non-Hertzian normal contact models, tangential contact, conformal contact	A modified version of Kalker's exact theory for solving conformal contact cases
Burgelman et al.[40] and Vollebregt et al.[41]	Non-Hertzian normal contact models, tangential contact, conformal contact	Integrated a conformal contact solution into the CONTACT algorithm
Pascal and Sauvage 1988[24]	Multi-Hertzian models	Contact jump modeling
Ayasse et al.[25]	Multi-Hertzian models	Pre-calculated tables and an analytical formulation for contact jump modeling
Kik and Piotrowski[36]	Virtual penetration models	Developed for better stress description in the contact patch and to be used directly in a multibody code (MEDYNA, ADAMS/Rail)
Liu et al.[30] EKP model	Virtual penetration models	Introduce the effect of wheelset yaw angle and variation in profile curvature across the contact patch.
Sun et al.[31] MKP model	Virtual penetration models	Relationship between the elastic deformation of a line and the normal pressure distribution.
Linder,[34] Ayasse and Chollet[33]	Virtual penetration models	Improve the virtual penetration method
Alonso and Giménez[42]	Non-steady state contact modeling	Proposed square root simplified theory to achieve elliptical pressure distribution.
Guiral et al.[43]	Non-steady state contact modeling	Improved the work by Alonso and Gimenez
Telliskivi[44]	Semi-Winkler approach	Account for the effect of neighboring material points which are connected by linear spring elements

Wheel-rail friction

Tangential contact models

Consider two elastic bodies in contact. If a torque is applied to one of the bodies a tangential force will be transmitted to the other body due to the friction in the contact patch and the bodies will roll over each other. The tangential contact problem consists in finding the tangential stress distribution, the tangential displacements, and the relative velocity in the contact patch.

Creepage and creep forces. The primary goal of the wheel-rail contact model is to calculate creep forces in the wheel-rail interface. Wheels are not only rolling on rails but also

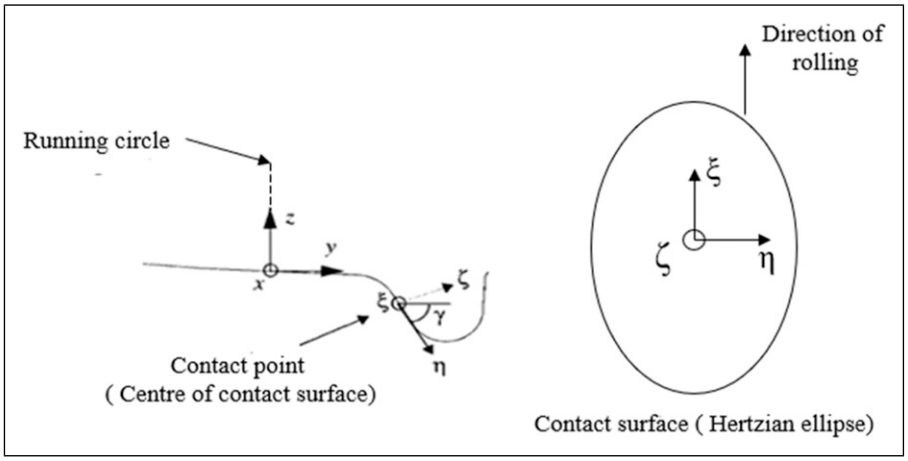

Figure 3. Coordinate system for the wheel profile (x-y-z) and the contact.[45]

sliding and spinning as well, especially during acceleration, braking, negotiating a curve, or when subjected to a lateral force. Frictional forces are generated at the wheel-rail interface due to differential tangential speeds at the contact interface. This differential speed can be normalized based on the absolute velocities of contacting bodies. In railroad terminology, the normalized differential speed is called creepage. Correspondingly, the actual, utilized friction forces and spin moments are commonly called the creep forces, where spin moments may be omitted if their effect is insignificant.

Creepage and spin are strongly affected by sliding velocity and angular velocity, while creep forces are affected by several factors including normal forces, coefficient of friction, material surface properties of the contacting bodies, wheel-rail geometry, and creepage and spin magnitudes.[45] Creepages can be categorized into three types; (1) longitudinal creepage (spinning and skidding), (2) lateral creepage (angle of attack or skew), and (3) spin creepage normal to the contact surface. Creep force, creepage, and sliding velocity are calculated using a coordinate system based on three axes (ξ-η-ζ)[45] as shown in Figure 3. where ξ is positive in the rolling direction, η is in the contact plane, and perpendicular to the travel direction, and ζ is perpendicular to the contact plane. Creepages in the longitudinal and lateral directions (υ_ξ, υ_η) are defined as the average sliding velocities (v_ξ and v_η) normalized by the vehicle speed (v vehicle). Spin (φ), on the other hand, is defined as the angular sliding velocity (ω) normalized by the vehicle speed. The total creepage, υ, is a vectorial sum of the longitudinal and the lateral creepages. Ayasse and Chollet[46] formulated general expressions for the creepage of two rolling bodies (wheel-rail on track or wheel-roller in a roller rig). Garg and Dukkipati[47,48] developed more general creepage formulations containing kinematics parameters of the wheelset, as well as considering the lateral radius of the rail.

Different theories have been proposed to solve the tangential contact problem. Kalker developed several wheel-rail contact theories that can be used to determine the tangential forces and spin moments between the wheel and the rail.[16] These theories are: Linear Theory, Strip Theory, Empirical Theory, Simplified Theory and Exact Three-Dimensional Rolling Contact Theory are all for non-conformal contacts, while Li and Kalker theories are for conformal contact solutions between the wheel and the rail. A concise summary of each theory as reported by Kalker is provided.

In general, tangential contact models can be divided into three types depending on their use: Fast and approximate approaches, such as the FASTSIM model,[49,64] FaStrip model,[50] and Polach's model.[51] The half-space-based approaches, specifically CONTACT, and models based on the table look-up scheme like the Kalker book of tables for non-Hertzian contact.[52] Numerical simulation methods like FEM and BEM can also be used for calculating both normal and tangential contact models.[53] They are discussed in Numerical simulation method

Kalker's theories

Linear theory. Kalker introduced the linear theory[54] in his PhD. dissertation, "On the Rolling Contact of Two Elastic Bodies in the Presence of Dry Friction." In this theory, the contact patch is divided into adhesion and sliding area, and the effect of the spin moment is included. The theory is based on the assumption that the distribution of traction at the leading edge of the contact is continuous. That is, the traction must vanish at the leading edge where the particles enter the contact area. On the other hand, within the contact area, the traction builds up until the trailing edge. The Linear theory is useful in many types of analysis simply because it is linear and given by explicit formulae. However, the theories produce larger errors as the shape of contact differs, for instance for a circular contact patch.[55] Moreover, the theory can only be applied to cases where the stick zone covers the entire contact patch, i.e., very small spin, and creepages. Kalker also made what is called Kalker's coefficients, which are a table of creepage and spin coefficients.[54]

Strip theory. The concept of employing a two-dimensional approach to solve a three-dimensional contact problem was first introduced by Haines and Ollerton[56] for the case of an elliptic contact patch subjected to longitudinal traction. Kalker extended the original Strip Theory developed by Haines and Ollerton[56] by employing lateral

and spin creepages in addition to longitudinal creepage. In this theory, the contact area is thought to be an ellipse with a long semi-axis. Kalker[54,57,58] proved that, for such contact areas, the area of contact can be divided into strips parallel to the longitudinal axis of the contact area. The strip theory was replaced by the Simplified Theory due to its limitation to slender contact area.

Empirical theory. Kalker introduced the Empirical Theory.[55] This theory defines the relationship between longitudinal and lateral creepages and total creep force. Kalker's empirical theory is more accurate compared to the empirical theory proposed by Vermeulen and Johnson in 1964.[13] The empirical theory can be used for all values of elastic constants of the two bodies.

The exact three-dimensional rolling contact theory. Kalker generalized the principle of virtual work for solving contact problems.[59,60] The exact Three-Dimensional Rolling Contact Theory was developed using the principle of virtual work. In this theory, the solution to the contact problem is determined by maximizing the complementary work over all possible functions that satisfy the constraints. In addition, the displacements of the surface in the contact area are expressed as integrals of the surface tractions by using influence functions.[16] The half-space assumption is used in this theory. Initially, the theory was incorporated into the DUVOROL contact program, and later into the well-known program CONTACT[16] to solve normal and tangential contact problems. The theory is not commonly used in multibody codes because the computational requirements for applying it are very high. as well as unsuitable for calculating each time step of the vehicle–track dynamics; therefore, the results obtained based on the CONTACT program are usually adopted to verify the accuracy of approximate calculation approaches for other engineering applications. CONTACT can be adapted to accurately calculate the contact patch shapes, contact stress distribution, and stick/slide distribution under any wheel-rail profiles. The exact 3D theory of Kalker is presently regarded as the benchmark against which other models are measured; it is the preferred solution for addressing the wheel-rail contact problem when computing time is not an issue. Several extensions have been developed that include the capability to treat conformal contact,[38–41] and the consideration of a third body layer in the wheel-rail interface[61] to the theory.

Simplified theory. Kalker developed the Simplified Theory.[49,62] The theory is based on approximating the relation between the tangential surface traction and the tangential surface displacement by using compliant (flexibility) parameters. These compliant parameters depend on the creepage and spin coefficients of the linear theory. This theory is used in the well-known program FASTSIM which was developed by Kalker in 1982.[49] FASTSIM uses normal contact problem solutions as input to calculate pressure distribution and creep forces of the contact area. FASTSIM is widely used in computer programs to determine the wheel-rail creep contact forces. The simplified theory can be used to investigate the influence of the surface layers that cover the bodies that are third-body particles at the contact surface.

Despite its advantages, FASTSIM presents certain limitations that have led different authors to modify the model to extend its applicability to non-elliptical contact areas. Some modifications are addressed to non-Hertzian contact that can be distinguished depending on how the flexibility parameters are computed like the equivalent ellipse methods[29,52,63] and direct methods[16,64] in which a different theory to Kalker's Linear Theory is used to compute the flexibility parameters for arbitrary contact areas. Recently Gómez-Bosch et al.,[65] modified the FASTSIM algorithm called the nH-FastSim, which is based on the direct method for calculating tangential forces and tractions over the wheel-rail contact area for non-Hertzian contact conditions and using the steady-state CONTACT version[16] assuming infinite friction coefficient for calculating flexibility parameters. The approach provides errors for creep forces less than 4% with computational times one order lower than the Variational Theory. Vollebregt and Wilders[66] refined the FASTSIM algorithm's discretization method to make it more accurate (or use fewer grid points for the same accuracy). Liu et al.[67] extend the generalization proposed by Vollebregt to compute the creep forces according to the linear theory for any Simple Double-Elliptic Contact (SDEC) shape. They did that by introducing four new coefficients for elliptic patches and maintaining the coefficients of the original linear theory to consider the effect of non-ellipticity in their model. The model is as fast as FASTSIM and provides more accurate solutions than existing versions of FASTSIM.

Li and kalker's theory. In the case of conformal contact, the half-space approximation is no longer valid as the size of the contact area is not small compared to the size of the contacting bodies. In addition, the creepages and spin are not constant within the contact area. Li and Kalker used two quasi-quarter spaces for solving the conformal contact problems.[39,68,69] In their approach, the variation of spin throughout the contact area is considered.

Johnson and vermeulen's theory. Johnson[70] proposed a rolling contact theory considering finite slip and neglecting the spin creepage for circular contacts. In his theory, the contact area is divided into two regions: the adhesion area (stick zone) which has a circular shape, and the slip zone which has the same direction as tangential stress. He also derives the relationships between creepages and creep forces. The theory is fast and more versatile than the linear theory but it is limited to state for pure longitudinal and lateral creep, i.e., spin = 0. Johnson[70] later considered the effect of spin showing that spin causes lateral creep force. Vermeulen and Johnson[13] later generalized the work for circular contact with elliptical contact using the solution for sliding contacts with micro slip.

The heuristic nonlinear creep force model. Several Heuristic models have been proposed including Ohayama,[71] Ayasse-Chollet-Pascal (under the name CHOPAYA), hyperbolic tangent, the arctangent,[72] and the Shen-Hedrick-Elkins models.[73] The Shen-Hedrick-Elkins model[73] is a

heuristic modification of Kalker's linear theory so that the friction law of Coulomb is fulfilled when the creepage is large i.e., designed to achieve a saturated regime. The result is that it can only be used for establishing a creep curve: it does not provide a good evaluation of what happens inside a contact patch, such as finding the slip, stress, or determining the location of the stick and slip zones. The model includes the effect of spin and can be expressed by:

$$F_{x_{NL}} = F_x \cdot \epsilon \tag{1}$$

$$F_{y_{NL}} = F_y \cdot \epsilon \tag{2}$$

where $F_{x_{NL}}, F_{y_{NL}}$ are the nonlinear longitudinal and lateral creep forces and ϵ is given by:

$$\epsilon = \begin{cases} \dfrac{\mu N}{F'_R}\left[\left(\dfrac{F'_R}{\mu N}\right) - \dfrac{1}{3}\left(\dfrac{F'_R}{\mu N}\right)^2 + \dfrac{1}{27}\left(\left(\dfrac{F'_R}{\mu N}\right)^2\right)\right] & \text{for } F'_R < 3\mu N \\ \dfrac{\mu N}{F'_R} & \text{for } F'_R < 3\mu N \end{cases} \tag{3}$$

where F'_R is the linear resultant creep force and N is the normal force to the contact plane.

Polach's contact model. Polach developed a fast algorithm and computer code for wheel-rail forces calculation.[51] The contact geometry, creep, and spin conditions are considered in this model. The assumption is based on a linear relationship between tangential deformation and traction. In this method, the creep forces are calculated firstly for a no-spin case, and then the spin case is considered. Polach[74] later extend the method to include the effects of falling friction and contaminants.

The calculation efficiency of the Polach model is higher than that of CONTACT and even FASTSIM, because it is more analytical than numerical i.e., having more elaborate friction laws. However, the calculation accuracy of this method is low in high spin creep conditions and does not provide an insight into the distribution of tractions in the contact area.[75]

Models based on the table look-up scheme. Table look-up approaches can be used to avoid long computation times. This approach is based on numerical solutions, but instead of solving the contact problem every time, many different contact situations are solved once and for all and then listed in a large table. To find the tangential force for a given contact situation it is thus a matter of interpolation in the table. The advantage of the table look-up approach is that the interpolation is much faster than computing the numerical solution.

British Rail developed the first Lookup table[76] for a parametrized elliptical contact patch, using Kalker's DUVOROL program.[77] As a result of pre-calculation time and computer storage limitations at the time, this table had four input parameters and a relatively small size with 3220 entries. Kalker later created a larger Lookup Table called USETAB[78] also based on the elliptical regularization of the contact patch. The table had 115 000 entries in which the stored creep forces were determined with the CONTACT software.[16] Later USETAB 1.2 was developed to accommodate 100 000 entries.[79] Commercial codes such as NUCARS and VAMPIRE are used in this improved version. The Kalker book of tables for non-Hertzian contact (KBTNH)[52,80,81] is the more recent development of the lookup table approach where a non-elliptical contact patch regularization has been suggested using five input parameters. The regularization assumes that the contact patch can be approximated by a single double elliptical contact region, which allows to capture the longitudinal creep force generated by the spin creepage. Two enhanced versions of the KBTNH are proposed by Marques et al.,[82] one that is approximately 5 times smaller than the original but maintains similar accuracy, and the other exhibiting half of the maximum interpolation error but holding an identical size. The KBTNH is suitable for wheels and rails with any profiles, including worn profiles and 7.8–51 times faster than FASTSIM working on 36–256 discretization elements, respectively when computing for creep forces.

Numerical simulation method

Finite element method analysis. The FEM is a numerical method for solving partial differential equations (PDEs). Partial differential equations are transformed into algebraic equations by removing spatial derivatives by discretizing the bodies under investigation into elements with a specific number of nodes, which are then analyzed. A wide range of material properties can be considered as there is no restriction on the half-space assumption of Hertz. Also, more detailed and advanced friction laws can be used.

Several contact problems involving rolling contact have been solved using FEM analysis.[53,83–88] Yan and Fischer[53] investigated the applicability of Hertz's theory in several wheel-rail contact situations using FEM. Wiest et al.[85] used FEM to investigate contact in switches. Telliskivi and Olofsson[87] investigated the effect of elasticity and half-space assumptions on contact solutions by comparing elasto-plastic (kinematic hardening) FEM results to those obtained by CONTACT and Hertz theory. A 3D transient FE model using an explicit time integration scheme was presented by Zhao and Li[88] for solving both normal and tangential contact problems simultaneously. Using Hertz's theory and Kalker's computer program CONTACT, they validate the normal and tangential solutions. Damme[86] developed an FEM model to analyze wheel-rail rolling contact using the arbitrary Lagrangian-Eulerian (ALE) approach. Finite Element Method often needs a long calculation time because of the need for a very fine mesh in the contact area.

Boundary element method analysis. Boundary Element Methods are a powerful alternative to FEM, particularly when better accuracy is required due to issues like stress concentration or when the domain extends to infinity. Several contact problems have been solved using BEM analysis.[4,89–92] Knothe and LeThe[90] proposed a contact model based on BEM. They divided the contact patch into strips while the contact pressure distribution in the rolling direction is assumed to be elliptical. Boundary Element Method is employed in Kalker CONTACT software.[4] The BEM is also employed in noise prediction of railway systems,[91] as well as in modeling boundary conditions to avoid wave reflections at the boundaries.[93]

In recent years, some researchers represented by Vollebregt[41,94–96] are developing wheel-rail conformal contact theories using the FEM. Some accelerating algorithms such as fast Fourier transform (FFTs)[97] are also employed to promote computation efficiency. The applicability of these theories in the vehicle system dynamic simulations remains to be investigated.

Contaminants at the wheel-rail contact

The tangential models discussed previously are utilized to calculate creep forces under dry wheel-rail contact. As previously stated, the wheel-rail contact is an open system exposed to environmental factors (contaminants, temperature, humidity, etc.) that influence adhesion, friction, and wear processes. The contaminants may be naturally occurring on the track (e.g., rain, snow, humidity, and biological materials like leaves and oxides) or purposefully introduced to the wheel-rail interface (e.g., lubricants/greases, traction gels, friction modifiers (FM)). Frictional processes between bodies in contact generate heat, which alters the properties of the surfaces in contact. The contaminants frequently found in wheel-rail contact, and their effects will be discussed here.

Water, oil, and leaves contaminants. The most common kind of natural contamination is rain or dew. Numerous studies have examined their effect on wheel-rail adhesion. Several studies have shown that water reduces wheel-rail adhesion,[98–100] but the exact mechanism is still unclear. There is some evidence that water reduces friction by facilitating the formation of iron oxides at the point of contact.[99] Wheel-rail contact is unlikely to be contaminated by water alone. Water influences the effects of other contaminants. Researchers have studied the joint effects of water and other contaminants.[99,101–103] For example, contacts with an oil and water mixture had a lower adhesion coefficient than a pure oil-lubricated contact.[99] Some studies suggest that water temperature affects friction and wheel-rail adhesion. The higher the water temperature the higher the friction.[104] Chang et al.[105] carried out measurements on a full-scale wheelset test rig, where they showed that the maximum adhesion coefficient decreases with an increase in speed and water spray. They also found that creepage increases with an increase in water temperature.

Numerous studies[106–109] have examined the effects of humidity on wheel-rail adhesion during traction or braking. It is believed that the coefficient of adhesion will decrease to a low value[107,108] in a high-humidity environment. Olofsson & Sundval[109] carried out a laboratory experiment that demonstrated that atmospheric humidity affects the traction coefficient of a dry rail (see Figure 4). When the wheel-rail interface is contaminated with leaves, humidity has little effect. Water also reduces wear rates.[110] The influence of precipitation on the rail wear rates measured from the field is shown in Figure 5. The low wear rate may be attributed to the reduction of friction due to water. The presence of water has been linked to a greater probability of RCF occurring.[111]

During autumn, leaves often fall onto railway tracks causing delays in train operation, isolation of wheels from a rail which may result in track circuit failure, and other related issues.[113,114] Under both dry and wet conditions, leaf layers have been reported to cause low wheel-rail adhesion. According to Olofsson and Sundvall,[109] leaf contamination of wheel-rail decreases friction coefficient by 0.3 in a dry environment and by 0.1 decreases in a humid environment. The aerodynamics of modern trains is such that leaves around the track are sucked to the wheel-rail contact and after several passes of the wheels, a series of chemical reactions occur leaving a black layer (Teflon-like layer) on the wheel-rail interface reducing adhesion. Cann[115] studied the problem of leaf residue and loss of adhesion in the wheel-rail surface using a ball-on-disc test device. The result shows that the leaves form a thin black layer on the disk thus its accumulation reduces friction and adhesion between the wheel and rail. Leaf layers can be removed using water jetting techniques, using lasers have also been investigated, or the use of sand or particle-based traction gels.

Friction modifiers at the wheel and rail contact. Today's rail networks are experiencing increased traffic levels, tighter running schedules, and increasing speed. The traction between the wheel and rail contact is an important issue. If it is too low the wheel slides rather than rolls; if it is too high then the wheel and rail are subject to excessive shear stress that leads to increased wear rates. To increase the service life of wheel and rail without compromising axle load and speed, it is necessary to increase the rail strength, decrease traction forces between rails and wheels, or introduce a third body that has anti-wear and anti-crack properties that reduces wear and RCF without reducing traction forces below the safety limits. This has seen the introduction and increasing use of FMs.

Friction modifiers are applied to the wheel-rail contact to control the traction coefficient in the contact to the desired level. Friction modifiers are also designed to tackle other rail-related issues, for example, reduce noise,[116] rail head corrugations, improve curving behavior, reduce ground-borne vibrations, as well as reducing wear and damage to both wheel and rail.[117] There is a wide range of FMs currently available on the market. They include a variety of additives that aid in achieving the desired level of friction (increase or decrease) in dry or contaminated conditions. The detailed constituents are not generally made public. Friction modifiers can be in the form of liquid (that subsequently dries once spread on the rail), solid, or a mixture (solid particles suspended in a gel). Special FMs were first introduced in the 1980s as solid FMs that reduced dry contact friction from a high to an intermediate level that is lower than dry rail but significantly higher than lubricated conditions.[118] Friction modifiers can be classified into three categories:[8]

- Low coefficient of friction modifiers (LCF): They have a friction coefficient of 0.2 or less and are mostly applied in the wheel flange rail gauge such as lubricants.

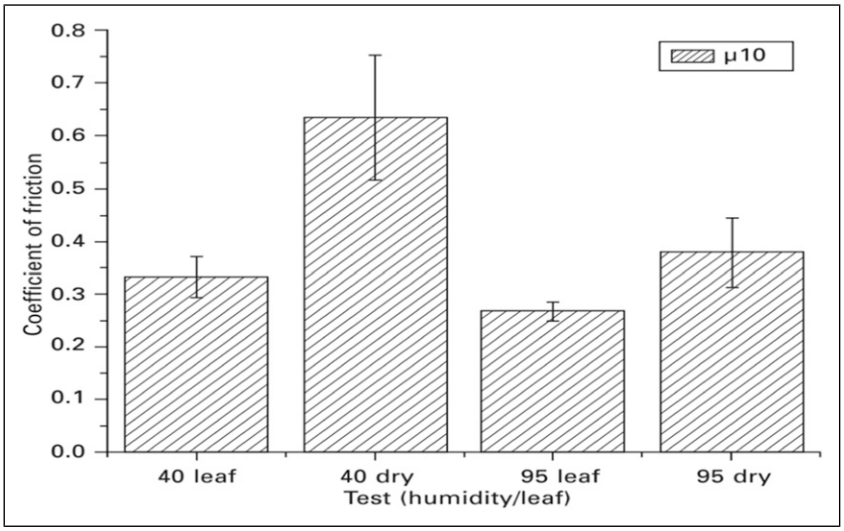

Figure 4. Influence of humidity on a dry and leaf-contaminated rail.[109]

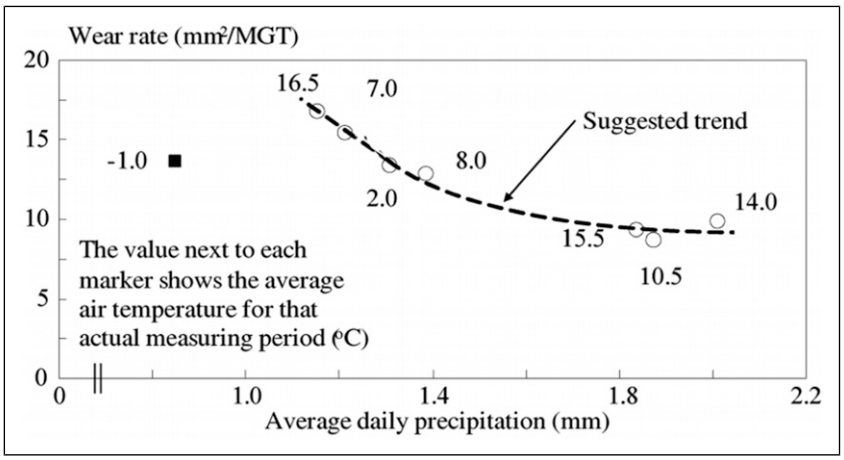

Figure 5. Influence of average daily precipitation on rail wear for a specific track site during various measuring periods.[112]
Note: MGT = mega gross tonne traffic. Note also the outlier at low temperatures.

- High positive coefficient friction modifiers (HPF):[119] Having friction coefficients of 0.2~0.4 which are used in wheel thread-TOR applications.
- Very high coefficient friction modifiers (VHPF): such as friction enhancers are used to increase adhesion for both traction and braking, for locomotives, or especially where adhesion loss problems occur. The main composition of the VHPF is sand. One of the side effects of using such a FM is that wear increases significantly.

Wheel-rail adhesion models

Many mathematical models for wheel-rail adhesion have been developed between real rough surfaces with contaminants such as water, oil, leaves, and so on. In earlier research, the effects of contaminants are considered by evaluating their friction coefficients from laboratory tests and importing them into the wheel-rail dry contact models.[120–122] However, this method can't handle the effects of liquid contaminants properly due to the mixed lubrication behavior at the interface. The contact area of two bodies with interfacial fluid can be separated into partly

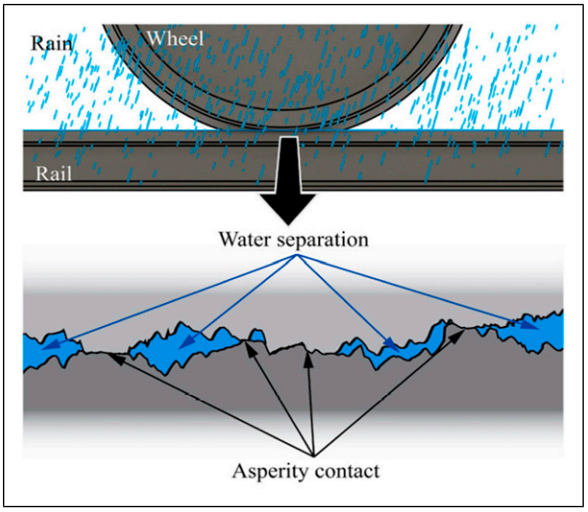

Figure 6. wheel-rail adhesion under water.[126]

contact of asperities and partly into areas where the fluid is separating both surfaces as shown in Figure 6. Some of the models used to calculate asperity contact include Bowden and Tabor adhesion model,[123] Greenwood and Tripp

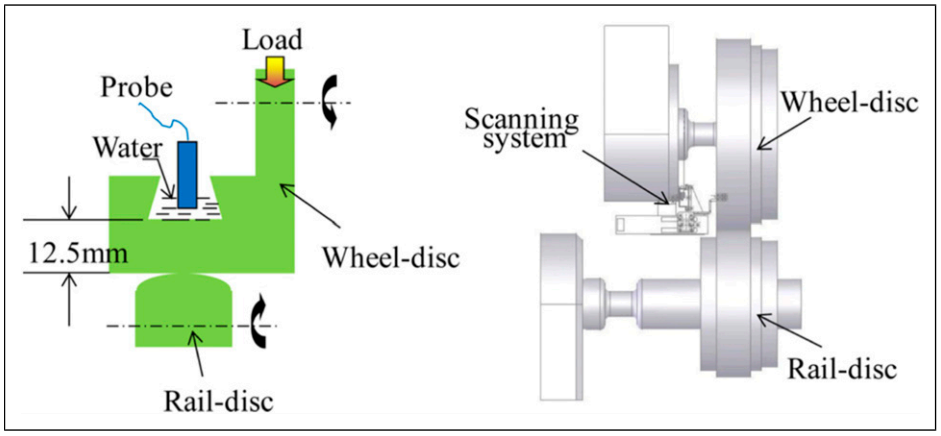

Figure 7. The twin-disc rolling contact machine equipped with an ultrasonic set-up.[133]

model,[124] etc. The elastohydrodynamic lubrication (EHL) theory[125] is introduced to evaluate the load carried by the fluid. These models take into account various parameters such as water, oil, leaves, surface roughness, etc. Current wheel-rail adhesion models will be explored in the next subsection.

Empirical adhesion models. Several methods have been used to investigate the influence of contaminants on the tribological properties at the wheel-rail interface including twin-disc experiments,[120,122,127–133] ball-on-disc measurement,[134] and field testing.[112] In early studies, Kalker's CONTACT and FASTSIM algorithms consider the influence of water by adjusting the constant values of the friction coefficient.[135,136] Some researchers[74,122,137] established empirical models for the wheel-rail adhesion ratios based on the experimental measurements (Figure 7).

Liu et al.[122] conducted a rolling contact twin disk testing to measure the lateral adhesion ratio under dry and wet conditions. Based on the experimental measurements, they established an empirical model that describes the relationship between the adhesion ratios and rolling speed which can provide a more precise description of the wheel-rail contact mechanics.

Trummer et al.[137] developed an empirical Water-induced low adhesion creep force model (WILAC) that is based on boundary lubrication theory to describe the wheel-rail adhesion in dry, moist, and wet conditions with special emphasis on moist conditions. The model can be implemented in multibody dynamics software or in braking models to study train performance and braking strategies. The WILAC model can predict the effect of water on wheel/rail adhesion in a wide range of conditions from dry, damp and wet conditions and agrees with existing locomotive test data from the literature.

Meacci et al.[138] presented a wheel-rail degraded adhesion model[138] that uses local sliding/creepages and pressures inside the contact area to describe the phenomena associated with the deterioration of adhesion between the wheel and rail. They improved and extended Kalker's FASTSIM algorithm to incorporate important phenomena such as the energy dissipated at the contact and surface cleaning effect, which results in a greater adhesion between wheel and rail. The model allows the achievement of a good trade-off between accuracy and numerical efficiency. Thus, the model can be embedded into multibody software to perform dynamic simulations at large scales.

Adhesion models based on the EHL theory. Fluids (water, oil, grease, etc.) make up the majority of the contaminants on the top of the track that could threaten the train's running safety. Whereas, the friction coefficient of wheel-rail under the fluids not only depends on the layer properties but also on the rolling velocity, external load, surface roughness, and so on. In rolling contact with fluids at the interface, the rolling motion and radial extrusion might cause hydrodynamic and boundary lubrication effects.[137]

Ohyama[125] and Chen et al.[139] are the scholars who earlier introduced the hydrodynamic lubrication theory[140] to study the adhesion problem with water in the wheel-rail interface. To reduce computation duration, EHL empirical equations[125,126,141] are employed to determine the adhesion coefficient directly in consideration of rough surfaces using the viscosity of water reported by Bett and Cappi.[142] Chen and her coworkers also[127] proposed an improved 3D numerical model using partial EHL theory at 3D contact to estimate the adhesion coefficient between wheel and rail by considering the surface roughness amplitude and roughness orientation parameters. Under wet conditions, numerical solutions obtained by the 3D numerical model are used to examine the effects of rolling speed, water temperature, roughness amplitude, and roughness orientation on asperity contact pressure, which influences adhesion coefficients significantly.

Wu et al.[143] and Wang et al.[144] developed a 2D numerical model of wheel-rail rolling contact under mixed oil/water contamination to study the adhesion characteristics of the wheels. In the model, partial EHL theory in line contact is applied. In mixed contamination conditions involving oil and water, the 2D numerical model is used to analyze how the contact pressures between the wheel and rail and the volume fraction of oil affect the adhesion coefficient.

Under the boundary lubrication regime, the load between wheel and rail is partially carried by the surface roughness peaks, and some asperity contact theories including Greenwood-Williamson (GW)[145,146] and Greenwood-Tripp (GT)[124] are applied to the computation of such load. The GW model treats the roughness of the

surface as an ensemble of identical spherical asperities, with randomly distributed heights. Using Kalker's simplified theory with an integrated third body layer, this model determines the frictional values of asperity contacts and the friction generated by liquids using the EHL theory. Greenwood-Williamson model has been widely employed, despite some of its limitations, such as the assumption of perfectly hemispherical asperity and constant asperity tip radius. The GT model is one of the first analytical solutions to model asperity contact, it has been applied by the following publications[143,147] for wheel-rail adhesion calculation with fluid interfacial layers and surface roughness. Statistical distributions of asperity heights and defined peaks are used in this approach. The contact pressure of asperities is calculated by using the mean asperity contact pressure compliance relationship which was developed based on the GW model.[141]

Concluding remark and research gaps

This paper presented a literature review of recent advances in wheel-rail contact and tribology theories and models. The wheel-rail contact is a typical tribological system with features that make the system unique and complicated. The review article first presents some basic information on wheel and rail contact and then explores methods to analyze wheel-rail contact including various Hertzian and non-Hertzian contact models. Next, the paper introduces the definition of creepage characteristics and investigates the theories and the wheel-rail friction models under dry and contaminated contact.

For the wheel-rail contact modeling approaches, the Hertzian contact models are still the most popular contact models due to their convenient implementation in multi-body dynamic code and acceptable computational duration. However, the Hertzian contact theory is not able to deal with the conformal and multi-point contact problems that frequently occur in the vicinity of the wheel flange regions. Exact non-Hertzian and numerical contact methods are computationally expensive when applied in the vehicle system dynamic analysis. The multi-Hertzian and virtual penetration models are the compromises between the Hertzian and exact non-Hertzian methods in terms of computational accuracy and efficiency. The contact between the wheel and rail is characterized by uneven geometric shapes and rough surfaces. Thus, numerical solutions and acceleration algorithms have to be pursued because no analytical solution is available in most practical cases.

The wheel-rail system is an open system that is exposed to water, humidity, leaves, and so on, accurately modeling the wheel-rail friction under the contaminated contact is still a challenge. The wheel-rail interfacial fluids, frictional heat, surface deformation, and oxidation complicate the physical-based mathematical modeling. Although the EHL theory is introduced to deal with these problems in recent decades, most work ignores the complex geometries and conformal contact near wheel flange and the solutions take a long time to achieve. Efficient and accurate wheel-rail adhesion models that integrate the non-Hertz contact formulas and EHL theories are required to provide a better understanding of the tribo-dynamic behavior of the wheel-rail system.

Declaration of conflicting interests

The author(s) declared no potential conflicts of interest with respect to the research, authorship, and/or publication of this article.

Funding

The author(s) disclosed receipt of the following financial support for the research, authorship, and/or publication of this article: The authors would like to thank the financial support from the National Key R&D Program of China (Grant no. 2020YFA0710902), National Natural Science Foundation of China (Grant nos. 51905549, 52130502), and Initial Funding of the Specially-appointed Associate Professorship of Central South University, China (Grant No. 202045009).

ORCID iDs

Congcong Fang https://orcid.org/0000-0002-9122-9059
Wei Zhou https://orcid.org/0000-0001-7767-3666
Xianghui Meng https://orcid.org/0000-0003-2387-1186

References

1. Burgelman N, Sichani MS, Enblom R, et al. Influence of wheel-rail contact modelling on vehicle dynamic simulation. *Veh Syst Dyn* 2015; 53: 1190–1203. DOI: 10.1080/00423114.2015.1039550
2. Shabana AA, Zaazaa KE and Sugiyama H. *Railroad vehicle dynamics: a computational approach*. Boca Raton, FL, CRC Press, 2008.
3. Eadie DT, Oldknow K, Santoro M, et al. Wayside gauge face lubrication: how much do we really understand? *Proc Inst Mech Eng F J Rail Rapid Transit* 2012; 227: 245–253. DOI: 10.1177/0954409712459306
4. Jacobson B and Kalker JJ. *Rolling contact phenomena*. Berlin, Germany, Springer, 2014.
5. Knothe K, Wille R and Zastrau BW. Advanced contact mechanics–road and rail. *Veh Syst Dyn* 2001; 35: 361–407.
6. Piotrowski J and Chollet H. Wheel-rail contact models for vehicle system dynamics including multi-point contact. *Veh Syst Dyn* 2005; 43: 455–483.
7. Meymand SZ, Keylin A and Ahmadian M. A survey of wheel-rail contact models for rail vehicles. *Veh Syst Dyn* 2016; 54: 386–428.
8. Olofsson U and Lyu Y. Open system tribology in the wheel-rail contact: a literature review. *Appl Mech Rev* 2017; 69: 060803. DOI: 10.1115/1.4038229
9. Soleimani H and Moavenian M. Tribological aspects of wheel-rail contact: a review of wear mechanisms and effective factors on rolling contact fatigue. *Urban Rail Transit* 2017; 3: 227–237.
10. Foo C, Omar B and Jalil A. A review on recent wheel/rail interface friction management. In: *Journal of physics: conference series*. IOP Publishing Limited, 2018, p. 012009.
11. Vollebregt E, Six K and Polach O. Challenges and progress in the understanding and modelling of the wheel-rail creep forces. *Veh Syst Dyn* 2021; 59: 1026–1068. DOI: 10.1080/00423114.2021.1912367
12. Carter FW. On the action of a locomotive driving wheel. *Proc Royal Society London Series A* 1926; 112: 151–157.

13. Vermeulen PJ and Johnson KL. Contact of nonspherical elastic bodies transmitting tangential forces. *J Appl Mech* 1964; 31: 338–340.
14. Kalker J. A strip theory for rolling with slip and spin. *Koninklijke Nederlandse Akademie Van Weteschappen-Proc Series B-PhysSci* 1967; 70: 10–24.
15. Salehi MFG. Stress analysis worn profiles based on Hertz theory. In: 20th Annual Conference of Mechanical Engineering. Tehran, Iran, 2012.
16. Kalker JJ. *Three-dimensional elastic bodies in rolling contact*. Dordrecht, Netherlands: Kluwer Academic Publishers, 2018.
17. Hertz H, Jones D and Schott G. *Miscellaneous papers*. London, UK: Macmillan, 1896.
18. Timoshenko S and Goodier J. *Theory of elasticity*. New York, NY, McGraw-Hill, 1951, p. 116.
19. Hamilton GM. Explicit equations for the stresses beneath a sliding spherical contact. *Proc Inst Mech Eng C J Mech Eng Sci* 1983; 197: 53–59.
20. Kalker J. Wheel-rail rolling contact theory. *Wear* 1991; 144: 243–261.
21. Baeza L, Vila P, Xie G, et al. Prediction of rail corrugation using a rotating flexible wheelset coupled with a flexible track model and a non-Hertzian/non-steady contact model. *J Sound Vib* 2011; 330: 4493–4507.
22. Kaiser I. Refining the modelling of vehicle–track interaction. *Veh Syst Dyn* 2012; 50: 229–243.
23. Xie G and Iwnicki SD. A rail roughness growth model for a wheelset with non-steady, non-hertzian contact. *Veh Syst Dyn* 2010; 48: 1135–1154.
24. Pascal J and Sauvage G. The available methods to calculate the wheel/rail forces in non hertzian contact patches and rail damaging. *Veh Syst Dyn* 1993; 22: 263–275.
25. Ayasse JB. Paramètres caractéristiques du contact roue-rail. Rapport INRETS 2000.
26. Pascal J-P and Soua B. Solving conformal contacts using multi-Hertzian techniques. *Veh Syst Dyn* 2016; 54: 784–813.
27. Sebès M, Chollet H, Ayasse J-B, et al. A multi-hertzian contact model considering plasticity. *Wear* 2014; 314: 118–124.
28. Sebès M, Chevalier L, Ayasse J-B, et al. A fast-simplified wheel-rail contact model consistent with perfect plastic materials. *Veh Syst Dyn* 2012; 50: 1453–1471.
29. Piotrowski J and Kik W. A simplified model of wheel/rail contact mechanics for non-Hertzian problems and its application in rail vehicle dynamic simulations. *Veh Syst Dyn* 2008; 46: 27–48.
30. Liu B, Bruni S and Vollebregt E. A non-hertzian method for solving wheel-rail normal contact problem taking into account the effect of yaw. *Veh Syst Dyn* 2016; 54: 1226–1246.
31. Sun Y, Zhai W and Guo Y. A robust non-hertzian contact method for wheel-rail normal contact analysis. *Veh Syst Dyn* 2018; 56: 1899–1921.
32. Sun Y and Ling L. An optimal tangential contact model for wheel-rail non-Hertzian contact analysis and its application in railway vehicle dynamics simulation. *Veh Syst Dyn* 2021; 60: 3240–3268.
33. Ayasse JB and Chollet H. Determination of the wheel rail contact patch in semi-hertzian conditions. *Veh Syst Dyna* 2005; 43: 161–172.
34. Linder C. *Verschleiss von Eisenbahnrädern mit Unrundheiten*. ETH Zurich, 1997.
35. Sichani MS, Enblom R and Berg M. A novel method to model wheel-railnormal contact in vehicle dynamics simulation. *Veh Syst Dyn* 2014; 52: 1752–1764.
36. Kik W and Piotrowski J. A fast, approximate method to calculate normal load at contact between wheel and rail and creep forces during rolling. In: 2nd mini-conference on contact mechanics and wear of rail/wheel systems, Budapest, 29-31 July, 1996, Warsaw Technical University.
37. Kalker JJ. Survey of wheel-rail rolling contact theory. *Veh Syst Dyn* 1979; 8: 317–358.
38. Li Z, Kalker J, Wiersma P, et al. Non-Hertzian wheel-rail wear simulation in vehicle dynamic systems [niet eerder opgevoerd]. In: *4th International Conference on Railway Bogies and Running Gears*. Budapest: Technical University of Budapest Dep. of Railway Vehicles, 1998, pp. 187–196.
39. Li Z. *Wheel-rail rolling contact and its application to wear simulation [PhD thesis]*. Delft, The Netherlands: Delft University, 2002.
40. Burgelman N, Li Z and Dollevoet R. A new rolling contact method applied to conformal contact and the train–turnout interaction. *Wear* 2014; 321: 94–105.
41. Vollebregt EAH. Conformal contact: corrections and new results. *Veh Syst Dyn* 2018; 56: 1622–1632.
42. Alonso A and Giménez JG. Non-steady state contact with falling friction coefficient. *Veh Syst Dyn* 2008; 46: 779–789.
43. Guiral A, Alonso A, Baeza L, et al. Non-steady state modelling of wheel-railcontact problem. *Veh Syst Dyn* 2013; 51: 91–108.
44. Telliskivi T. Simulation of wear in a rolling–sliding contact by a semi-winkler model and the archard's wear law. *Wear* 2004; 256: 817–831.
45. Jendel T. *Prediction of wheel and rail wear: a pilot study ISRN KTH/FKT//FR-99/03-SE*. Stockholm, Sweden: Royal Institute of Technology, 1999.
46. Ayasse J-B and Chollet H. *Wheel-railcontact, handbook of railway vehicle dynamics*. ISBN-13 2006: 970–978.
47. Dukkipati RV. *Vehicle dynamics*. Boca Raton, FL: CRC Press, 2000.
48. Garg V. *Dynamics of railway vehicle systems*. Amsterdam, Netherlands: Elsevier, 2012.
49. Kalker JJ. A fast algorithm for the simplified theory of rolling contact. *Veh Syst Dyn* 1982; 11: 1–13.
50. Sh Sichani M, Enblom R and Berg M. An alternative to FASTSIM for tangential solution of the wheel-rail contact. *Veh Syst Dyn* 2016; 54: 748–764.
51. Polach O. A fast wheel-rail forces calculation computer code. *Veh Syst Dyn* 1999; 33: 728–739.
52. Piotrowski J, Liu B and Bruni S. The Kalker book of tables for non-Hertzian contact of wheel and rail. *Veh Syst Dyn* 2017; 55: 875–901.
53. Yan W and Fischer FD. Applicability of the Hertz contact theory to rail-wheel contact problems. *Arch Appl Mech* 2000; 70: 255–268.
54. Kalker JJ. *On the rolling contact of two elastic bodies in the presence of dry friction*. Delft, Netherlands: Delft University of Technology, 1967.
55. Kalker JJ. The tangential force transmitted by two elastic bodies rolling over each other with pure creepage. *Wear* 1968; 11: 421–430. DOI: 10.1016/0043-1648(68)90551-6
56. Haines DJ and Ollerton E. Contact stress distributions on elliptical contact surfaces subjected to radial and tangential forces. *Proc Inst Mech Eng* 1963; 177: 95–114.

57. Kalker J. The transmission of force and couple between two elastically similar rolling spheres. *Proc KNAW– Amsterdam* 1964; B67: 135–177.
58. Kalker JJ. On elastic line contact. *J Appl Mech* 1972; 39: 1125–1132. DOI: 10.1115/1.3422841
59. Kalker JJ. The principle of virtual work and its dual for contact problems. *Ing Arch* 1986; 56: 453–467. DOI: 10.1007/BF00533832
60. Kalker JJ. Numerical calculation of the elastic field in a half-space. *Commun Appl Numer Methods* 1986; 2: 401–410. DOI: 10.1002/cnm.1630020412
61. Vollebregt EA. 100-fold speed-up of the normal contact problem and other recent developments in" CONTACT. In: Proceedings of the 9th International Conference on Contact Mechanics and Wear of Rail/Wheel Systems China, Chengdu, China, 2012, pp. 201–209.
62. Kalker JJ. *Simplified theory of rolling contact*. Delft, The Netherlands: Delft University of Technology, 1973.
63. Alonso A and Giménez JG. Tangential problem solution for non-elliptical contact areas with the FastSim algorithm. *Veh Syst Dyn* 2007; 45: 341–357. DOI: 10.1080/00423110600999763
64. Knothe K and Hung L-T. A method for the analysis of the tangential stresses and the wear distribution between two elastic bodies of revolution in rolling contact. *Int J Solids Struct* 1985; 21: 889–906. DOI: 10.1016/0020-7683(85)90040-X
65. Gómez-Bosch J, Giner-Navarro J, Carballeira J, et al. A direct method for the extension of FastSim under non-Hertzian contact conditions. *Veh Syst Dyn* 2022; 1–19. DOI: 10.1080/00423114.2022.2120022
66. Vollebregt EAH and Wilders P. FASTSIM2: a second-order accurate frictional rolling contact algorithm. *Comput Mech* 2011; 47: 105–116. DOI: 10.1007/s00466-010-0536-7
67. Liu B, Fu B and Bruni S. Generalisation of the linear theory of rolling contact to a single double-elliptic contact region and its application to solve non-Hertzian contact problems using extended FASTSIM. *Veh Syst Dyn* 2022; 1–19. DOI: 10.1080/00423114.2022.2113808
68. Li L and Kalker J. The computation of wheel-rail conformal contact. In: Proceedings of the 4th World Conference on Computational Mechanics Buenos Aires. Argentina, June-July 1998.
69. Li LZ and Kalker JJ. *The computation of wheel-rail conformal contact computational mechanics, new trends and applications*. Idelsohm S, Onate E and Dvorkin E (eds). Barcelona, Spain: CIMME, 1998.
70. Johnson K. *The effect of a tangential contact force upon the rolling motion of an elastic sphere on a plane*, 1958, pp. 332–338.
71. Ohyama T. Some problems of the fundamental adhesion at higher speeds. *Q Rep RTRI* 1973; 14: 181–187.
72. Simon I, Cole C and McSweeney T (eds). *Handbook of railway vehicle dynamics*. 2nd Edition. Boca Raton, FL: CRC Press, 2019.
73. Shen ZY, Hedrick JK and Elkins JA. A comparison of alternative creep force models for rail vehicle dynamic analysis. *Veh Syst Dyn* 1983; 12: 79–83.
74. Polach O. Creep forces in simulations of traction vehicles running on adhesion limit. *Wear* 2005; 258: 992–1000. DOI: 10.1016/j.wear.2004.03.046
75. Vollebregt EAH, Iwnicki SD, Xie G, et al. Assessing the accuracy of different simplified frictional rolling contact algorithms. *Veh Syst Dyn* 2012; 50: 1–17. DOI: 10.1080/00423114.2011.552618
76. Rose K. Kalker table for wheel/rail force prediction. In: *Internal memorandum IM VTI*. UK: British Rail Research Derby, 1984.
77. Kalker JJ. *Introduction to the FORTRAN 14 programs Duvorol and contact for the solution of 3 D elastostatic half-space contact problems with and without friction*, 1982.
78. Kalker JJ. *Book of tables for the herzian creep-force law*. Delft University of Technology, Faculty of Technical Mathematics and Informatics, 1996.
79. Vollebregt E. Refinement of Kalker's rolling contact model. In: *Proceedings of the 8th International Conference on Contact Mechanics and Wear of Rail/Wheel Systems*. Firenze, Italy: Citeseer, 2009, pp. 149–156.
80. Escalona JL, Yu X and Aceituno JF. Wheel-railcontact simulation with lookup tables and KEC profiles: a comparative study. *Multibody Syst Dyn* 2021; 52: 339–375.
81. Piotrowski J, Bruni S, Liu B, et al. A fast method for determination of creep forces in non-Hertzian contact of wheel and rail based on a book of tables. *Multibody Syst Dyn* 2019; 45: 169–184.
82. Marques F, Magalhães H, Liu B, et al. On the generation of enhanced lookup tables for wheel-rail contact models. *Wear* 2019; 434-435: 202993.
83. Akama M. Development of finite element model for analysis of rolling contact fatigue cracks in wheel/rail systems. *QR of RTRI* 2007; 48: 8–14.
84. Srivastava JP, Sarkar PK and Ranjan V. Contact stress analysis in wheel-railby Hertzian method and finite element method. *J Inst Eng India Ser C* 2014; 95: 319–325.
85. Wiest M, Kassa E, Daves W, et al. Assessment of methods for calculating contact pressure in wheel-rail/switch contact. *Wear* 2008; 265: 1439–1445.
86. Damme S. *Zur finite-element-modellierung des stationären rollkontakts von rad und schiene*. Ph.D. thesis, Inst. für Mechanik und Flächentragwerke, Technischen Universität Dresden, 2006.
87. Telliskivi T and Olofsson U. Contact mechanics analysis of measured wheel-rail profiles using the finite element method. *Proc Inst Mech Eng F J Rail Rapid Transit* 2001; 215: 65–72.
88. Zhao X and Li Z. The solution of frictional wheel-rail rolling contact with a 3D transient finite element model: validation and error analysis. *Wear* 2011; 271: 444–452.
89. Qazi A, Yin H, Sebès M, et al. A semi-analytical numerical method for modelling the normal wheel-rail contact. *Veh Syst Dyn* 2022; 60: 1322–1340.
90. Knothe K and Le The H. A contribution to the calculation of the contact stress distribution between two elastic bodies of revolution with non-elliptical contact area. *Comput Struct* 1984; 18: 1025–1033.
91. Yang X. *Theorical analysis and control studies in wheel/rail noise of high speed railway*. Chengdu, China: Southwest Jiaotong University, 2010.
92. Andersson T. The boundary element method applied to two-dimensional contact problems with friction. In: *Boundary element methods*. Berlin, Germany: Springer, 1981, pp. 239–258.

93. Zhai W, Wei K, Song X, et al. Experimental investigation into ground vibrations induced by very high speed trains on a non-ballasted track. *Soil Dyn Earthquake Eng* 2015; 72: 24–36.
94. Vollebregt E and Segal G. Solving conformal wheel-rail rolling contact problems. *Veh Syst Dyn* 2014; 52: 455–468. DOI: 10.1080/00423114.2014.906634
95. Blanco-Lorenzo J, Santamaria J, Vadillo EG, et al. On the influence of conformity on wheel-rail rolling contact mechanics. *Tribol Int* 2016; 103: 647–667. DOI: 10.1016/j.triboint.2016.07.017
96. Vollebregt E. Detailed wheel/rail geometry processing with the conformal contact approach. *Multibody Syst Dyn* 2021; 52: 135–167.
97. Polonsky IA and Keer LM. Fast methods for solving rough contact problems: a comparative study. *J Tribol* 2000; 122: 36–41.
98. Wang W, Zhang H, Wang H, et al. Study on the adhesion behavior of wheel/rail under oil, water and sanding conditions. *Wear* 2011; 271: 2693–2698.
99. Lewis R, Gallardo-Hernandez EA, Hilton T, et al. Effect of oil and water mixtures on adhesion in the wheel/rail contact. *Proc Inst Mech Eng F J Rail Rapid Transit* 2009; 223: 275–283.
100. Buckley-Johnstone L, Trummer G, Voltr P, et al. Full-scale testing of low adhesion effects with small amounts of water in the wheel/rail interface. *Tribol Int* 2020; 141: 105907.
101. Arias-Cuevas O, Li Z, Lewis R, et al. Rolling–sliding laboratory tests of friction modifiers in dry and wet wheel-railcontacts. *Wear* 2010; 268: 543–551.
102. Zhu Y, Chen X, Wang W-j, et al. A study on iron oxides and surface roughness in dry and wet wheel− rail contacts. *Wear* 2015; 328-329: 241–248.
103. White B, Kempka R, Laity P, et al. Iron oxide and water paste rheology and its effect on low adhesion in the wheel/rail interface. *Tribol Lett* 2022; 70: 8–14.
104. Chen H, Ban T, Ishida M, et al. Effect of water temperature on the adhesion between rail and wheel. *Proc Inst Mech Eng J J Eng Tribol* 2006; 220: 571–579.
105. Chang C, Chen B, Cai Y, et al. An experimental study of high speed wheel-rail adhesion characteristics in wet condition on full scale roller rig. *Wear* 2019; 440-441: 203092.
106. Rong K-j, Xiao Y-l, Shen M-x, et al. Influence of ambient humidity on the adhesion and damage behavior of wheel-railinterface under hot weather condition. *Wear* 2021; 486-487: 204091.
107. Lyu Y, Zhu Y and Olofsson U. Wear between wheel and rail: a pin-on-disc study of environmental conditions and iron oxides. *Wear* 2015; 328-329: 277–285.
108. Zhu Y, Lyu Y and Olofsson U. Mapping the friction between railway wheels and rails focusing on environmental conditions. *Wear* 2015; 324-325: 122–128.
109. Olofsson U and Sundvall K. Influence of leaf, humidity and applied lubrication on friction in the wheel-rail contact: pin-on-disc experiments. *Proc Inst Mech Eng F J Rail Rapid Transit* 2004; 218: 235–242.
110. Hardwick C, Lewis R, Eadie D, et al. Rail wear–understanding the effect of third body materials. In: Proceedings of the IoM3 Conference on 20th Century Rail. New York, UK, 2011, pp. 1–3.
111. Fletcher DI, Hyde P and Kapoor A. Investigating fluid penetration of rolling contact fatigue cracks in rails using a newly developed full-scale test facility. *Proc Inst Mech Eng F J Rail Rapid Transit* 2007; 221: 35–44.
112. Nilsson R. *On wear in rolling/sliding contacts*. Ph. D. thesis. Sweden: Royal Institute of Technology KTH, 2005.
113. Arias-Cuevas O and Li Z. Field investigations into the adhesion recovery in leaf-contaminated wheel-railcontacts with locomotive sanders. *Proc Inst Mech Eng F J Rail Rapid Transit* 2011; 225: 443–456.
114. Arias-Cuevas O, Li Z, Lewis R, et al. Laboratory investigation of some sanding parameters to improve the adhesion in leaf-contaminated wheel—rail contacts. *Proc Inst Mech Eng F J Rail Rapid Transit* 2010; 224: 139–157.
115. Cann P. The “leaves on the line” problem—a study of leaf residue film formation and lubricity under laboratory test conditions. *Tribol Lett* 2006; 24: 151–158.
116. Eadie DT, Elvidge D, Oldknow K, et al. The effects of top of rail friction modifier on wear and rolling contact fatigue: full-scale rail–wheel test rig evaluation, analysis and modelling. In: Proceedings 7th International Conference on Contact Mechanics and Wear of Rail/Wheel Systems Brisbane, QLD, Australia: 24–27 September, 2006, pp. 411–419.
117. Suda Y, Iwasa T, Komine H, et al. Development of onboard friction control. *Wear* 2005; 258: 1109–1114.
118. Kalousek J and Johnson KL. An investigation of short pitch wheel and rail corrugations on the Vancouver mass transit system. *Proc Inst Mech Eng F J Rail and Rapid Transit* 1992; 206: 127–135.
119. Kalousek J and Magel E. Modifying and managing friction. *Railw Track Struct* 1997; 5–6.
120. Zhang W, Chen J, Wu X, et al. Wheel/rail adhesion and analysis by using full scale roller rig. *Wear* 2002; 253: 82–88.
121. Wu B, Xiao G, An B, et al. Numerical study of wheel/rail dynamic interactions for high-speed rail vehicles under low adhesion conditions during traction. *Eng Failure Analysis* 2022; 137: 106266. DOI: 10.1016/j.engfailanal.2022.106266
122. Liu X, Xiao C and Meehan PA. The effect of rolling speed on lateral adhesion at wheel/rail interface under dry and wet condition. *Wear* 2019; 438-439: 203073. DOI: 10.1016/j.wear.2019.203073
123. Bowden FP and Tabor D (eds). *The friction and lubrication of solids*. New York: Clarendon Press, 1958.
124. Greenwood JA and Tripp JH. The contact of two nominally flat rough surfaces. *Proc Inst Mech Eng* 1970; 185: 625–633.
125. Ohyama T. Tribological studies on adhesion phenomena between wheel and rail at high speeds. *Wear* 1991; 144: 263–275.
126. Kvarda D, Galas R, Omasta M, et al. Asperity-based model for prediction of traction in water-contaminated wheel-rail contact. *Tribol Int* 2021; 157: 106900. DOI: 10.1016/j.triboint.2021.106900
127. Chen H, Ishida M and Nakahara T. Analysis of adhesion under wet conditions for three-dimensional contact considering surface roughness. *Wear* 2005; 258: 1209–1216. DOI: 10.1016/j.wear.2004.03.031

128. Chen H, Fukagai S, Sone Y, et al. Assessment of lubricant applied to wheel-rail interface in curves. *Wear* 2014; 314: 228–235. DOI: 10.1016/j.wear.2013.12.006
129. Hardwick C, Lewis R and Eadie DT. Wheel and rail wear-Understanding the effects of water and grease. *Wear* 2014; 314: 198–204. DOI: 10.1016/j.wear.2013.11.020
130. Six K, Meierhofer A, Müller G, et al. Physical processes in wheel-rail contact and its implications on vehicle–track interaction. *Veh Syst Dyn* 2014; 53: 635–650. DOI: 10.1080/00423114.2014.983675
131. Omasta M, Machatka M, Smejkal D, et al. Influence of sanding parameters on adhesion recovery in contaminated wheel-rail contact. *Wear* 2015; 322-323: 218–225. DOI: 10.1016/j.wear.2014.11.017
132. Shi LB, Ma L, Guo J, et al. Influence of low temperature environment on the adhesion characteristics of wheel-rail contact. *Tribol Int* 2018; 127: 59–68. DOI: 10.1016/j.triboint.2018.05.037
133. Chen H, Ishida M, Namura A, et al. Estimation of wheel/rail adhesion coefficient under wet condition with measured boundary friction coefficient and real contact area. *Wear* 2011; 271: 32–39. DOI: 10.1016/j.wear.2010.10.022
134. Kvarda D, Skurka S, Galas R, et al. The effect of top of rail lubricant composition on adhesion and rheological behaviour. *Eng Sci Tech Int J* 2022; 35: 101100.
135. Spiryagin M, Polach O and Cole C. Creep force modelling for rail traction vehicles based on the Fastsim algorithm. *Veh Syst Dyn* 2013; 51: 1765–1783. DOI: 10.1080/00423114.2013.826370
136. Vollebregt EAH. Numerical modeling of measured railway creep versus creep-force curves with CONTACT. *Wear* 2014; 314: 87–95. DOI: 10.1016/j.wear.2013.11.030
137. Trummer G, Buckley-Johnstone LE, Voltr P, et al. Wheel-rail creep force model for predicting water induced low adhesion phenomena. *Tribol Int* 2017; 109: 409–415. DOI: 10.1016/j.triboint.2016.12.056
138. Meacci M, Shi Z, Butini E, et al. A local degraded adhesion model for creep forces evaluation: an approximate approach to the tangential contact problem. *Wear* 2019; 440-441: 203084. DOI: 10.1016/j.wear.2019.203084
139. Chen H, Yoshimura A and Ohyama T. Numerical analysis for the influence of water film on adhesion between rail and wheel. *Proc Inst Mech Eng J J Eng Tribol* 1998; 212: 359–368.
140. Pinkus O and Sternlicht SA. *Theory of hydrodynamic lubrication*. New York, NY: McGraw-Hill, 1961.
141. Chen H, Ban T, Ishida M, et al. Adhesion between rail/wheel under water lubricated contact. *Wear* 2002; 253: 75–81.
142. Eisenberg D and Kauzmann W. *The structure and properties of water*. Oxford, New York: OUP Oxford, 2005.
143. Wu B, Wen Z, Wang H, et al. Numerical analysis on wheel/rail adhesion under mixed contamination of oil and water with surface roughness. *Wear* 2014; 314: 140–147.
144. Wang H, Wang WJ and Liu QY. Numerical and experimental investigation on adhesion characteristic of wheel/rail under the third body condition. *Proc Inst Mech Eng J J Eng Tribol* 2015; 230: 111–118. DOI: 10.1177/1350650115591232
145. Johnson K and Greenwood J. An adhesion map for the contact of elastic spheres. *J Colloid Interface Sci* 1997; 192: 326–333.
146. Greenwood JA, Williamson JBP and Bowden FP. Contact of nominally flat surfaces. *Proc Royal Society of London Series A* 1966; 295: 300–319. DOI: doi:10.1098/rspa.1966.0242
147. Tomberger C, Dietmaier P, Sextro W, et al. Friction in wheel-rail contact: a model comprising interfacial fluids, surface roughness and temperature. *Wear* 2011; 271: 2–12.